UAV ICING TRIALS: A NEW APPROACH

Iris David Du Mutel de Pierrepont Franzetti, Politecnico di Torino & EURAC Research, Italy
Arrigo Avi, Politecnico di Milano, Milano, Italy
Elisa Capello, Politecnico di Torino, Turin, Italy
Giuseppe Quaranta, Politecnico di Milano, Milano, Italy
Riccardo Parin, EURAC Research, Bolzano, Italy

Abstract

The experimental analysis of ice formation on multirotor propellers is proposed in this work. The effect of cloud droplet size and liquid water content is tested at different temperature conditions to examine the ice structure formation. Single rotor experiments have been conducted for 10”x4.7” and 15”x5” propellers at -2º C and -12º C making use of an icing wind tunnel inside a climatic chamber for the simulation of realistic icing conditions. A force-torque sensor is used for the performance evaluation of the propellers in terms of thrust and torque during the ice accretion. The objective of this work is the characterization of the ice formation based on cloud characteristics together with the study of the ice shedding phenomenon that entails abrupt performance changes. The resulting experimental data can be used as a reference for thrust loss estimation and required power computation aimed at planning real-life UAV missions in alpine environments.

1. NOTATION

Symbols

F_z	Thrust along z axis [N]
P_E	Electric power [W]
P_M	Mechanical power [W]
T_z	Torque around z axis [Nm]

Acronyms:

UAV	Unmanned Aerial Vehicle
IPS	Icing Protection System
MVD	Mean Volume Droplets
LWC	Liquid Water Content
LEC	Large Environmental Chamber
PWM	Pulse Width Modulation

2. INTRODUCTION

Icing on aviation is a well-known phenomenon for airplanes as well as for rotorcraft and it is well covered by regulations within EASA CSs [1]. The case of Unmanned Aerial Vehicles (UAV) has not yet been covered in legislation. UAVs are a powerful tool in outdoor environments, allowing for coverage of deserted areas and payload transport between remote locations, however extreme climates can be challenging for these vehicles. Flying in icing conditions could represent a significant overload to the platform with the consequent failure of the planned mission and loss of the vehicle.

Figure 1. Icing wind tunnel

In 2018 the European Union adopted a new Unmanned Aircraft Systems (UAS) regulatory framework, which is a proportional risk-based approach to UAS. This rule identified three categories of operation: basic, specific and certified [2]. The category specific requires authorization by the competent authority that goes through the definition of the Specific Operation Risk Assessment (SORA), which defines the SAIL (Specific Assurance and Integrity Level. When SAIL is IV or higher a specific Design Verification Process (DVP) is required, as indicated in Ref [3]. So, if a risk of flight in icing conditions is foreseen it must be shown that the vehicle is either able to sustain these conditions safely, or has means to detect and avoid or safely exit those conditions [4].

Figure 2. Single-rotor test setup

Consequently, testing of UAV aircraft, in environments where it will be possible also to test flight qualities and so assess the capability to perform exit manoeuvres may speed up significantly the increase of operations classified as SAIL IV or higher.

The experimental testing of icing conditions for fixed-wing UAVs has always been a popular topic of research due to their resemblance to airplanes. In [5], an icing wind tunnel is used for the evaluation of glaze, rime and mixed ice types for medium-sized fixed-wing UAVs. Low air speeds were considered from 25 m s^{-1} up to 40 m s^{-1}. Besides manual tracings, photogrammetry and laser scanner studies were conducted to capture the ice shapes. In [6], fixed-wing propeller performance degradation is studied and a model that describes such process is proposed. In [7], an Icing Protection System (IPS) is proposed. In the case of multi-copters, the experimental approach to icing conditions is a very recent topic of research. Typically studied from a numerical point of view [8], the performance evaluation of a single-rotor is measured in [9] using a fixed testbed and a weight sensor. In [10] an IPS is proposed based on single rotor measurements conducted on a one axis force sensor. A multi-layered electrothermal IPS was layered across the propeller blades and tested against rime and glaze ice conditions, proving to be particularly effective on the latter. The need for an effective IPS for multi-rotors is becoming evident as the flight space of these vehicles continuously expands, being shared in some cases with bigger and better equipped aircraft. For this end, a highly thorough experimental assessment of the phenomenon is due. Realistic environmental conditions need to be experimentally tested to ensure validation and approval of proposed anti-icing solutions so that the future deployment in real UAV platforms is as safe and reliable as possible. In [11], propeller performance was studied inside the LEC changing temperature and pressure levels down to -40º C and down to 300 hPa, respectively. The work is later completed with full quadcopter tests [12]. In [13], free flights at high altitude (pressure values corresponding to 0 m up to 9000 m) are performed using a quadrotor and different payload weights. In the present manuscript, we present the new ice wind tunnel developed in terraXcube and preliminary characterized in [14] in terms of Mean Volume Droplets (MVD) and Liquid Water Content (LWC) as proposed by ARP 5905 [15]. First trials on single propeller (10”x4.7” and 15”x5” propellers) with glaze and rime ice conditions at constant MVD or LWC have been performed. The preliminary experimental campaign aims to define and propose a new approach on testing UAVs under icing conditions adapting EASA specifications to these smaller but more versatile aerial vehicles.

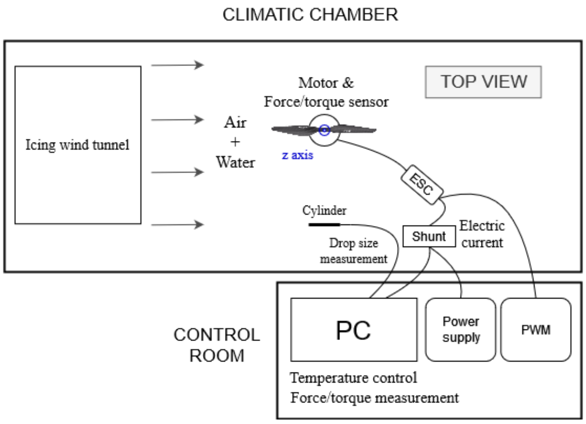

Figure 3. Experimental test setup

3. EXPERIMENTAL SETUP

Tests are conducted at terraXcube, EURAC Research, Bolzano in a 360 m^3 climatic chamber that allows changes in pressure and temperature that go from 1013 hPa down to 300 hPa and -40º C to 60º C, respectively. For this study, pressure is not controlled and temperature is changed to create different icing conditions. For this purpose, the rotor configurations are placed centered and at the height of the outlet of the icing wind tunnel (*Figure 2*). A general scheme of the complete experimental setup can be seen in *Figure 3*.

3.1. Icing wind tunnel

The icing wind tunnel at terraXcube (*Figure 1*) has been recently developed specifically for testing group 1 and 2 UAVs following the EASA CSs – Appendix C regulation. The setup regulates the subcooled liquid cloud in terms of air speed, MVD, LWC on a 2.5 m^3 volume. A complete description of the icing wind tunnel can be found in [16].

3.2. Single rotor and sensors

Table 1 Single propeller setup components

Component	Model
Motor	T-Motor MN3508-29 KV:380
ESC	T-Motor 40A Air
Propellers	10”x4.7” carbon fiber T-Motor 15”x5” carbon fiber Polish
Force-torque sensor	JR3 30E12A4
Tachometer	WLA16P-24162100A00
Power supply	APM SP-1U/2U

The test setup consists of a fixed structure to which a 6 degrees-of-freedom (6 DOF) force-torque sensor is fixed. The load cell is able to measure forces and torques with a resolution of 0.05 N for F_z , the force in the z axis and 0.002 Nm for T_z, the torque in the same axis. The z axis of the sensor is aligned with the vertical direction and thus with the propeller's thrust direction. The current draw of the motor is measured at the power cables of the ESC using a precision shunt resistor. The motor is powered using a power supply at two different voltages: 14.8 V for 10”x4.7” propellers and 22.2 V for 15”x5” propellers, as indicated by the motor manufacturer. The tachometer is set to record the rotation speed of the propeller and is powered with an independent power supply. During icing tests, the tachometer was not able to provide reliable data due to the formation of ice on its lens. The sensors and components can be found in *Table 1*.

4. METHODOLOGY

Single propeller tests were performed at a constant air speed of 10 m s^{-1} for two temperature levels: -2º C and -12º C. An equal LWC and MVD are set for both experiments with LWC = 1.2 g m^{-3} ± 0.2 g m^{-3} and a droplet size of 36 µm ± 3 µm. The test is performed at constant PWM signal and a minimum of one motor stop is performed during measurements as a check point for the correct operation of all equipment. A sample frequency of 10 Hz is set for the collection of all data.

5. RESULTS

Forces and torques can be seen in *Figure 4* for icing experiments of 10”x4.7” and 15”x5” propellers. Glaze ice condition has been tested at -2º C, while rime ice was obtained at -12º C. Since a different supply voltage and PWM command was given to the motor for

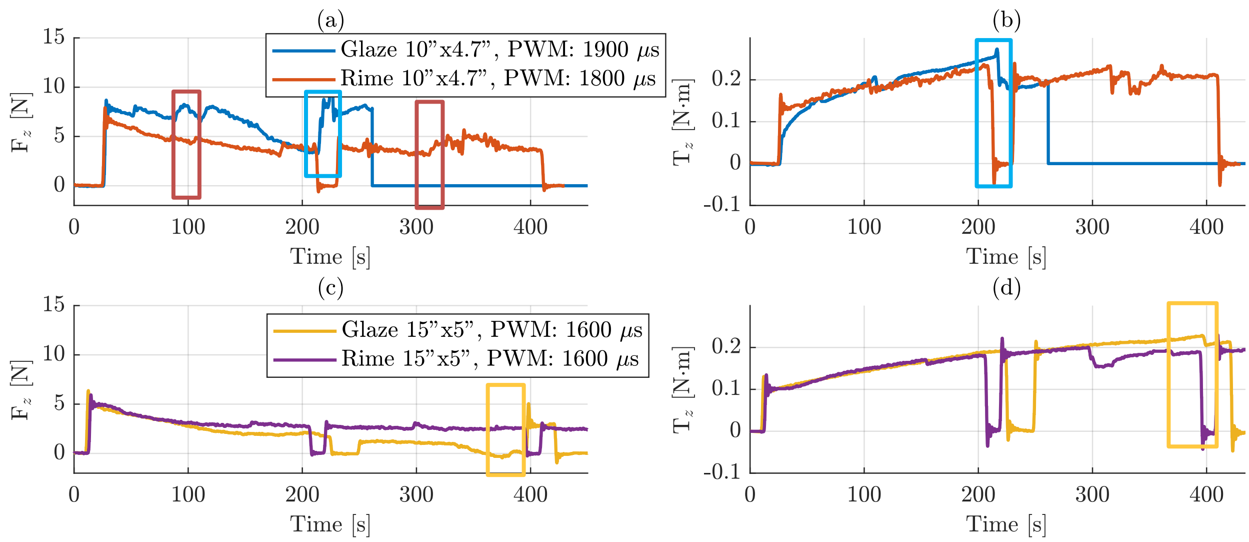

Figure 4. Single propeller icing experiments: Force (F_z) and torque (T_z) from glaze and rime ice formations on 10“x4.7“ and 15“x5“ propellers. Shedding occurrences are marked by rectangular markers colored accordingly to match the data referenced. LWC = 1.2 g m^{-3} ± 0.2 g m^{-3} and MVD = 36 µm ± 3 µm.

Table 2 No ice condition

Propeller	P_E [W]	P_M [W]	PWM [µs]	RPM [rev/min]	Fz [N]
10”x4.7”	107	94	1800	6800	6.6
	173	130	1900	7200	10
15”x5”	66	41	1600	3900	5.1

the two propeller models, thrust, torque and rotation speed are not equal. In *Table 2*, an ideal no-ice condition is presented to be used for comparison. In the warmer case, the droplets freeze after sliding over the surface of the propeller, forming glaze ice that can be seen in *Figure 5*.

In the lower temperature case shown in *Figure 6*, the

$$F_{z\ Loss}(\%) = \frac{F_{z_{ideal}} - F_{z_{ice}}}{F_{z_{ideal}}} \cdot 100 \quad (1)$$

droplets freeze on impact with the surface and therefore the accumulation of ice takes place at the stagnation point creating rime ice. The thrust is affected in

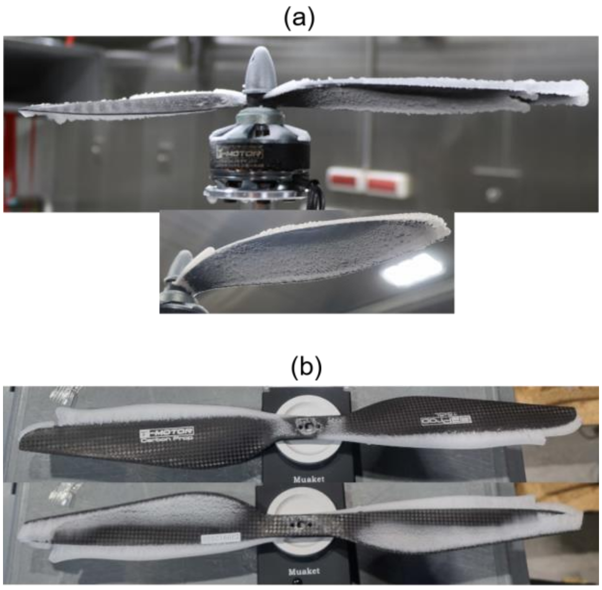

Figure 6. Rime ice on (a) 10“x4.7“ and (b) 15“x5“ propellers

both cases, being more critical in the case of glaze ice. The thrust loss ($F_{z\ Loss}$) is computed as in equation *(1)*, where $F_{z_{ideal}}$ are the values of thrust in the no ice condition reported in *Table 2*, and $F_{z_{ice}}$ are thrust values obtained from the data in *Figure 4*. For a 10” propeller, a maximum loss of 67% of the thrust is measured during glaze ice experiments. The same propeller during rime ice tests experiences a maximum loss of thrust of 53%. Glaze ice on the 15” propeller modifies the aerodynamic profile in such a way that no thrust is produced whatsoever at second 380

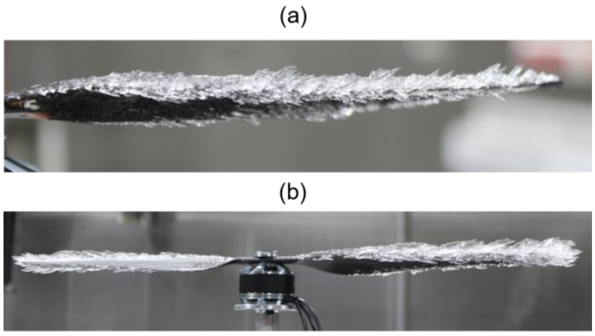

Figure 5. Glaze ice on (a) 10“x4.7“ and (b) 15“x5“ propellers

of the experiment. Rime ice on the 15” propeller causes a thrust decrease of 50% by the end of the test. Due to the higher temperatures and different accumulation processes, pieces of the formation often come off from the surface during operation times (ice shedding phenomenon). In *Figure 4* (a) and (b), some shedding can be seen for the glaze ice condition at second 210, in which the thrust and the torque are suddenly re-established. In *Figure 4* (c) and (d), this phenomenon takes place around second 380 of the experiment, where thrust is briefly improved as the propeller is momentarily free of residue. It must be noted that the shedding phenomenon is related to the ice accumulation as well as the rotation speed of the

$$P_M = \Omega \cdot T \qquad P_E = V \cdot I \quad (2)$$

propellers. The fastest speed and higher vibration of the 10” propellers justify a more frequent occurrence of this phenomenon. Decreasing propeller diameter implies higher rotation speeds and therefore more frequent shedding. Even though rime ice affects the aerodynamics less severely, ice residue shedding is not as usual as in the case of glaze ice, causing a steady growth of the ice formations. Some shedding can be seen for 10” propellers in the rime ice test at seconds 100 and 310 in *Figure 4* (a) and (b). However, the thrust values reported in *Figure 4* for rime ice formations and the two propeller models show a steadier decreasing tendency due to the less frequent shedding occurrence, when compared to the glaze ice test results. The behavior of the torque is inverse to that of the thrust, increasing with the accumulation of ice.

The accumulation of ice has a direct impact on the electric power P_E posing a challenge during battery powered flights. The current draw is increased proportionally to the torque, as the drag grows due to the ice build-up. In the case of no ice, the electric power consumed is reported in *Table 2*. The electric power consumed during icing conditions are reported in *Table 3*.

Table 3 Electric power on icing conditions. P_{E1} is measured at the beginning of the test, P_{E2} is the maximum value reached during the test.

Propeller	Ice conditions	P_{E1} [W]	P_{E2} [W]
10”x4.7”	Glaze	168	259
	Rime	103	194
15”x5”	Glaze	41.5	109
	Rime	43	86

The presence of rime ice approximately doubles the electric power consumed for both propeller types. For glaze ice, the maximum power consumed for the 15” propellers is scaled by a factor of 2.62 with respect to the power consumed at the beginning of the test. For smaller propellers, where ice sheds more often, the maximum power is 1.5 times the power at the start of the test. These results indicate that the size of the propeller has a non-negligible impact on the required power of the rotor based on the icing formation types.

6. CONCLUSIONS

The results presented in this work comprise single 10” and 15” rotor experiments for two different icing conditions, that are compared to an ideal no-ice situation. An analysis of the forces and torques depending on the ice formations over the propeller is introduced. The phenomenon of ice shedding from the propeller surface is also introduced and discussed based on the experimental data collected, concluding that rotation speed and ice type influence the shedding periodicity and impact on performance. Glaze ice tends to shed more frequently due to the lower temperature and irregular formation of the ice. Moreover, a higher rotation speed incites more frequent occurrences. The slower rotation of bigger propellers causes a steadier ice accretion with less frequent shedding, therefore a more stable behavior is expected from bigger rotors. Smaller propellers can cause a multirotor vehicle to be unstable due to the unpredictable shedding events. Overall, the aerodynamic performance of the propeller is deteriorated by the fast formation of ice in both cases, being particularly disruptive in the case of glaze ice. This experimental application can be used as reference for ice modelling and numerical simulation validation. The shedding phenomenon is of high interest, as it could be modelled and predicted based on ice and rotor characteristics. As future lines of work, tests will be conducted using a quadcopter to analyze the imbalances in forces and torques suffered on a fully equipped multirotor. Also, the mechanical power of the rotors will be analyzed to assess the efficiency of each propeller type under icing conditions.

Author contact:

Iris David Du Mutel de Pierrepont Franzetti iris.daviddu@polito.it

Arrigo Avi arrigo.avi@polimi.it

Elisa Capello elisa.capello@polito.it

Giuseppe Quaranta giuseppe.quaranta@polimi.it

Riccardo Parin riccardo.parin@eurac.edu

7. ACKNOWLEDGMENTS

We would like to thank Andrea Eccher and the team at terraXcube for their support during the experiments.

8. REFERENCES

[1] Easa, “Easy Access Rules for Large Rotorcraft (CS-29) (Amendment 6),” 2019.

[2] European Union Basic Regulation, “(EU) 2018/1139”.

[3] EASA, “Guidelines on Design verification for UAS operated in the ‘specific’ category,” Issue 3, 26 September 2023.

[4] EASA, “Special Condition Light Unmanned Aircraft Systems-Medium Risk Special Condition for Light Unmanned Aircraft Systems-Medium Risk“. 17 December 2020.

[5] R. Hann, “UAV Icing: Ice Accretion Experiments and Validation,” *SAE Technical Papers*, vol. 2019-June, no. June, Jun. 2019, doi: 10.4271/2019-01-2037.

[6] N. C. Müller and R. Hann, "UAV Icing: A Performance Model for a UAV Propeller in Icing Conditions," *AIAA AVIATION 2022 Forum*, 2022, doi: 10.2514/6.2022-3903.

[7] R. Hann *et al.*, "Experimental Investigations of an Icing Protection System for UAVs," *SAE Technical Papers*, vol. 2019-June, no. June, Jun. 2019, doi: 10.4271/2019-01-2038.

[8] A. Tramposch, M. Thomann, and D. Kozomara, "Determination of Droplet Impingement on an Octocopter at different Flight and Icing Conditions with CFD Methods," *AIAA Aviation and Aeronautics Forum and Exposition, AIAA AVIATION Forum 2021*, 2021, doi: 10.2514/6.2021-2501.

[9] P. Pecho, M. Jarosova, P. Fodor, and J. Rostas, "Experimental Analysis of the Effect of Icing an Unmanned Aerial Vehicles In Multicopter Configuration," *New Trends in Civil Aviation*, vol. 2022-October, pp. 147–151, 2022, doi: 10.23919/NTCA55899.2022.9934427.

[10] N. Karpen, S. Diebald, F. Dezitter, and E. Bonaccurso, "Propeller-integrated airfoil heater system for small multirotor drones in icing environments: Anti-icing feasibility study," *Cold Reg Sci Technol*, vol. 201, Sep. 2022, doi: 10.1016/j.coldregions.2022.103616.

[11] M. Scanavino, A. Vilardi, and G. Guglieri, "An Experimental Analysis on Propeller Performance in a Climate-controlled Facility," *Journal of Intelligent and Robotic Systems: Theory and Applications*, vol. 100, no. 2, pp. 505–517, Nov. 2020, doi: 10.1007/s10846-019-01132-9.

[12] M. Scanavino, A. Avi, A. Vilardi, and G. Guglieri, "Unmanned Aircraft Systems Performance in a Climate-Controlled Laboratory," *Journal of Intelligent and Robotic Systems: Theory and Applications*, vol. 102, no. 1, May 2021, doi: 10.1007/s10846-021-01392-4.

[13] R. Parin, A. Bojeri, F. Benedetto, G. Ristorto, and G. Guglieri, "Unmanned Aerial Vehicles Experimental Characterization in Controlled Extreme Environmental Conditions," *2023 International Conference on Unmanned Aircraft Systems, ICUAS 2023*, pp. 658–662, 2023, doi: 10.1109/ICUAS57906.2023.10155932.

[14] A. Avi, G. Quaranta, and R. Parin, "New UAV ice tunnel characterization," *MATERIALS RESEARCH PROCEEDINGS*, vol. 37, pp. 258–261, 2023.

[15] Society of Automotive Engineers, "Calibration and Acceptance of Icing Wind Tunnels," *SAE-ARP 5905*, 2015.

[16] A. Avi, L. Becce, G. Quaranta, F. Mazzetto, and R. Parin, "Characterization of the Spray System of the TerraXcube Icing Wind Tunnel," *Aerotecnica Missili & Spazio*, 2024, doi: 10.1007/s42496-024-00224-6.